SSCL-295

Temperature Rise in the Beam Tube During a Quench Due to the Eddy Currents and Related Effects

G. López

Accelerator Division
Superconducting Super Collider Laboratory*
2550 Beckleymeade Avenue
Dallas, TX 75237

July 1990

* Operated by the Universities Research Association, Inc., for the U.S. Department of Energy under Contract No. DE-AC02-89ER40486.

SSCL-295

Temperature Rise in the Beam Tube During a Quench Due to the Eddy Currents and Related Effects

G. López

Abstract

The eddy-current effects calculations are incorporated into the quench computer programs for the Superconducting Super Collider. The temperature rise in the beam tube and related effects are studied for passive and active protection systems.

CONTENTS

FIGURES

1.0 INTRODUCTION

When a quench appears in a dipole magnet, the magnetic field drops quite rapidly, in approximately 0.4 sec. It induces eddy currents in the surface of the beam tube, thereby creating a magnetic field that tries to compensate for the changes of the field, on the surface, according to Faraday's law.[1] In fact, this happens any time the magnetic field changes (during ramping or turning off the power supply), but the fastest change occurs only in the event of a quench. The main effects of these eddy currents are the Lorentz forces, and the temperature rise in the beam tube. This temperature is axially uniform along the beam tube which is enclosed by the magnet, as the borders of the magnet are not considered. Part of the stored energy in the magnet is dissipated in the beam tube wall, raising its temperature. If this temperature is too high, there could be a transmission of heat through the warmed helium to different parts of the coil in the same magnet, or even to the next magnet, with a potential to cause other quenches.

The forces and the temperature rise depends on the copper-plated thickness of the inner-beam wall. It is likely to have the thickness as large as possible (low-wall impedance considerations) in order for the parasitic heating (wake-field power loss) and low multi-bunch growth rate[2] to be low. The upper limit of the thickness is determined by the maximum induced force allowed in the beam tube, during a quench, that maintains the mechanical integrity of the beam pipe.

Although there have been several studies about eddy currents (see Reference 3), it is natural to incorporate these studies, in quench computer programs, to study their effects under different situations (passive or active protection system). Using the computer program for the Superconducting Super Collider (SSC), the results of the eddy-current effects for passive and active protection systems are presented in this report.

2.0 EDDY-CURRENT DENSITY

Consider a cylindrical beam tube of inner radius "b", outer radius "a", and with a copper-plated thickness Δ, shown in Figure 1. The eddy-current density distribution can be calculated using Ohm's law,

$$\mathbf{E} = \rho\, \mathbf{J}\ , \tag{1}$$

and integrating Faraday equations

$$\nabla \times \mathbf{E} = -\frac{\partial \mathbf{B}}{\partial t} \tag{2}$$

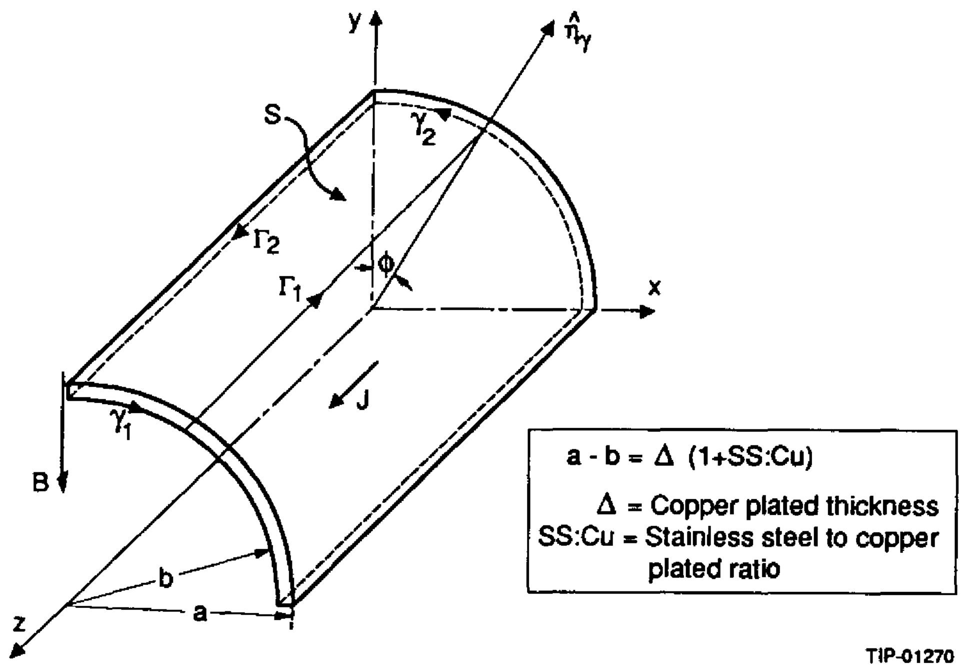

Figure 1. One Quarter of the Cylindrical Beam Tube.

on surface S as shown in Figure 1, where ρ is the copper resistivity, $\mathbf{J}$ is the vector-current density, $\mathbf{E}$ is the electric field, and $\mathbf{B}$ is the magnetic field. Using Equation (1) and Stokes' theorem in the integration, it follows that

$$\rho \int_{\partial S} \mathbf{J} \cdot \hat{n}_l \, , dl = -\frac{d}{dt} \int_S \mathbf{B} \cdot \hat{n}_r da \, , \tag{3}$$

where ∂S is the boundary of surface S, which is given in terms of their paths as

$$\partial S = \gamma_2 + \Gamma_2 + \gamma_1 + \Gamma_1 \, , \tag{4}$$

$\hat{n}_l$ and $\hat{n}_r$ are unitary vectors, pointing to the paths and radial direction, respectively. Assume magnetic field $\mathbf{B}$ is only time-dependent with components given by

$$\mathbf{B} = (0, -B, 0) \, , \tag{5}$$

and the angle made by $\mathbf{B}$ and $\hat{n}_r$ is given by $\pi - \phi$. The vector current density $\mathbf{J}$ is orthogonal to $\hat{n}_l$ in paths γ_1 and γ_2 (the borders of the magnet are not included), and are zero at path Γ_2, and also remains constant in the opposite direction to $\widehat{n}_l$, in path Γ_1. Using these conditions in Equation (3), the current density follows after some arrangements are made:

$$J = -\frac{b\dot{B}}{\rho} sin(\phi) \; , \tag{6}$$

where $\dot{B}$ is the variation of the magnetic field with time.

3.0 FORCE AND PRESSURE INDUCED ON THE BEAM TUBE

The density of force in the beam pipe is given by

$$\frac{d\mathbf{F}}{dv} = \mathbf{J} \times \mathbf{B} \; , \tag{7}$$

where dv is the differential of volume in the beam pipe. This force is pointing outward in the "x" direction, and the non-zero component of the density of force can be written using Equation (6) as

$$\frac{dF_x}{dv} = -\frac{bB\dot{B}}{\rho} sin(\phi) \; . \tag{8}$$

The force per-length per-angle is obtained by integrating Equation (8) in the radial direction, resulting in the following relation:

$$\frac{d^2F_x}{dzd\phi} = -\frac{b^2 \Delta B\dot{B}}{2\rho} sin(\phi) \; ; \tag{9}$$

its radial component, $\left(\frac{d^2F_x}{dzd\phi}\right)_r$, is given by

$$\left(\frac{d^2F_x}{dzd\phi}\right)_r = -\frac{b^2 \Delta B\dot{B}}{2\rho} sin^2(\phi) \; . \tag{10}$$

The pressure on the right side of the beam tube, p, can be obtained integrating Equation (10) with respect to the angle from 0 to $\pi/2$, dividing by "b" and multiplying by 2 (two quarters), thus obtaining this result:

$$p = -\frac{b\Delta B\dot{B}}{\rho}\frac{\pi}{4} \; . \tag{11}$$

4.0 TEMPERATURE ON THE BEAM TUBE WALL

The temperature rise in the beam tube, θ, can be calculated from the following equation:

$$(\delta C)(\theta)\frac{d\theta}{dt} = \left(1 + \frac{\rho}{\rho_{ss}}\right)\rho J^2 \, , \tag{12}$$

where ρ and ρ_{ss} are the resistivities of the copper and stainless steel, respectively, θ is the uniform temperature along the axial direction of the beam tube, and (δC) is the product of the density times the specific heat averaged over the components of the beam tube. The copper resistivity depends on the residual resistivity ratio (RRR), temperature (θ), and magnetic field (B):

$$\rho = \rho_{RRR}(\theta, B) \; . \tag{13}$$

Using Equation (6) in Equation (12), the temperature can be calculated, solving the following equation:

$$(\delta C)(\theta)\frac{d\theta}{dt} = -\left(1 + \frac{\rho_{RRR}(\theta, B)}{\rho_{ss}}\right)\frac{b^2\dot{B}^2}{\rho_{RRR}(\theta, B)} sin^2(\phi) \; . \tag{14}$$

The expressions (6), (9), (11) and (14) are coupled through the copper resistivity function (13) and should not be solved independently.

5.0 RESULTS

Using the computer programs at SSC, the magnetic field and the variation of the magnetic field with time can be known, since these are linearly related with the current flowing in the coil. A typical variation of the current flowing in the magnet with time, when the quench appears, at the pole-tip-turn of the inner coil in a 50 mm SSC R&D dipole magnet, is shown in Figure 2.

The eddy-current, the force-per-length, and the temperature rise at the midplane ($\phi = \pi/2$) as well as the pressure in a half of the beam tube are calculated solving the coupled-system presented by Equations (6), (9), (11), (13) and (14), and using the following parameters:

$$b = 22.25 \text{ mm} , \tag{15_a}$$

$$\Delta = 0.05 \text{ mm} , \tag{15_b}$$

$$SS : CU = 21 , \tag{15_c}$$

$$RRR = 30 . \tag{15_d}$$

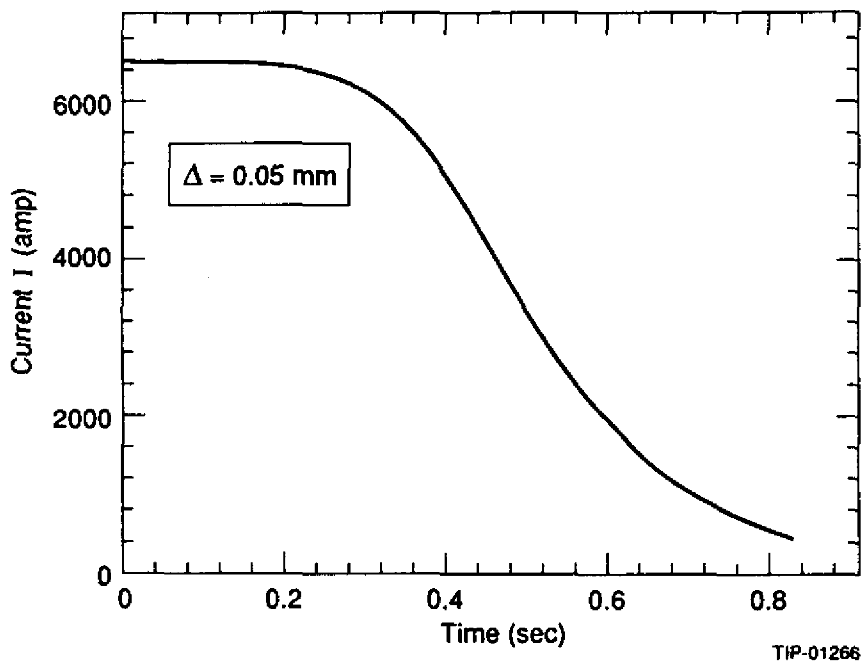

Figure 2. Current Decays During a Quench.

Figure 3 shows the eddy current induced during a quench. Figure 4 shows the force-per-length changes with time. The pressure evolution in half of the beam tube is shown in Figure 5, and the temperature rise, as a function of time, is shown in Figure 6. These calculations were made assuming a passive protection system for a single 50 mm SSC R&D dipole magnet.

If an active protection system is implemented, as it was pointed out in Reference 4, the time delay for the heaters to cause quenches must be quite brief (less than 50 ms). Assuming that two magnets are protected by heaters[5] and that a quench appears in one of them, the question concerns changes occurring in the peak values (as shown in Figures 3,

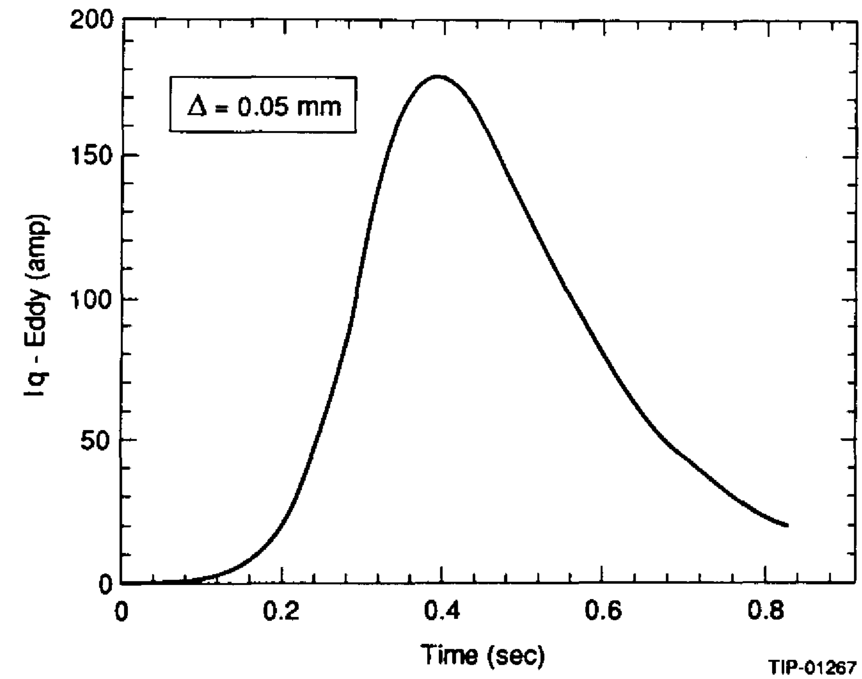

Figure 3. Eddy Current Induced at the Midplane of the Beam Tube.

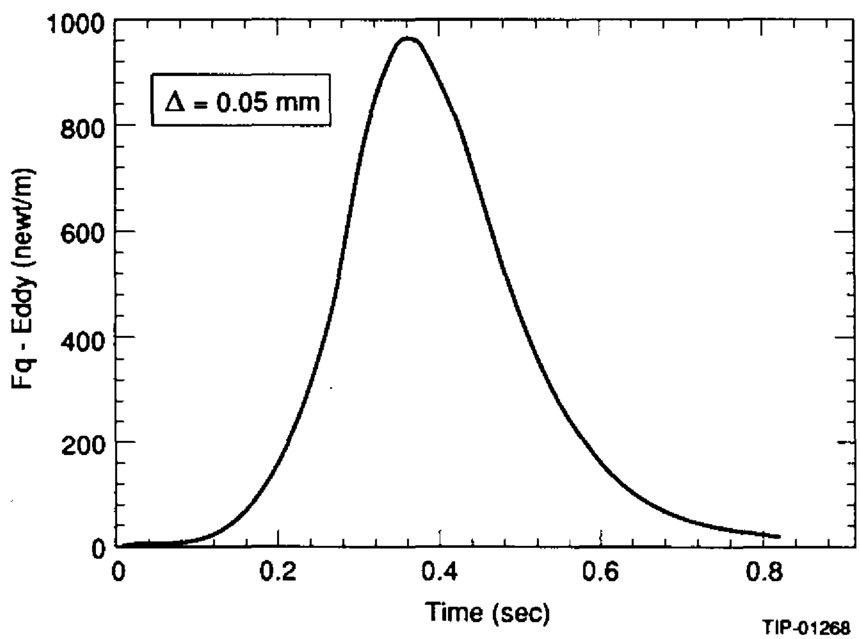

Figure 4. Lorentz's Force per Length at the Midplane of the Beam Tube.

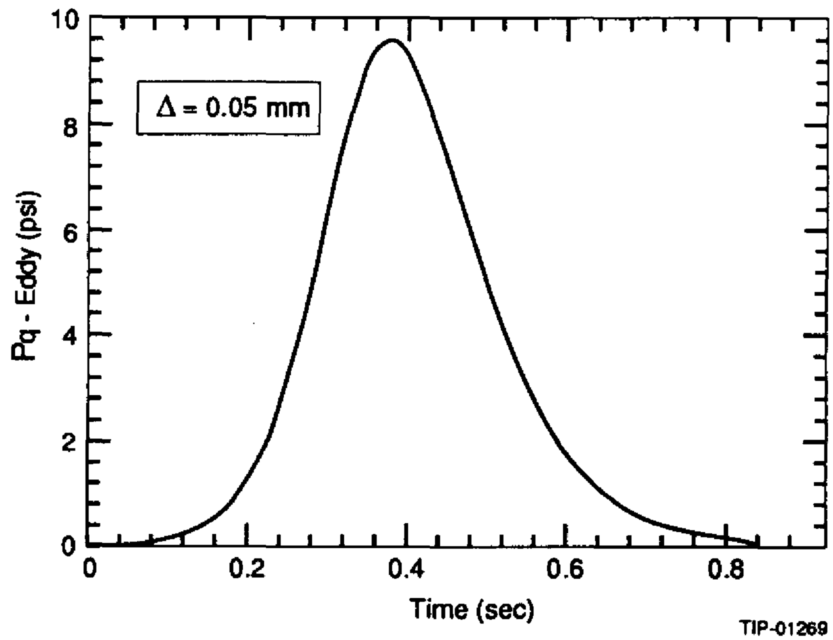

Figure 5. Pressure in a Half of the Beam Tube.

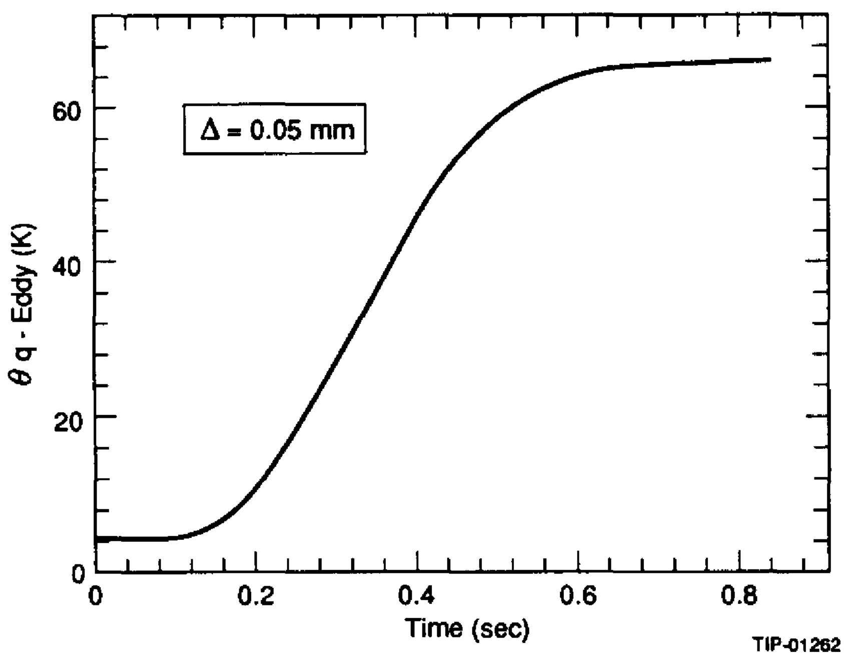

Figure 6. Temperature Rise at the Midplane of the Beam Tube.

4, 5 and 6) as a function of heater time delay. As shown in Figure 7, there are no significant changes when heater time delay, τ_h, is between 5 and 45 ms.

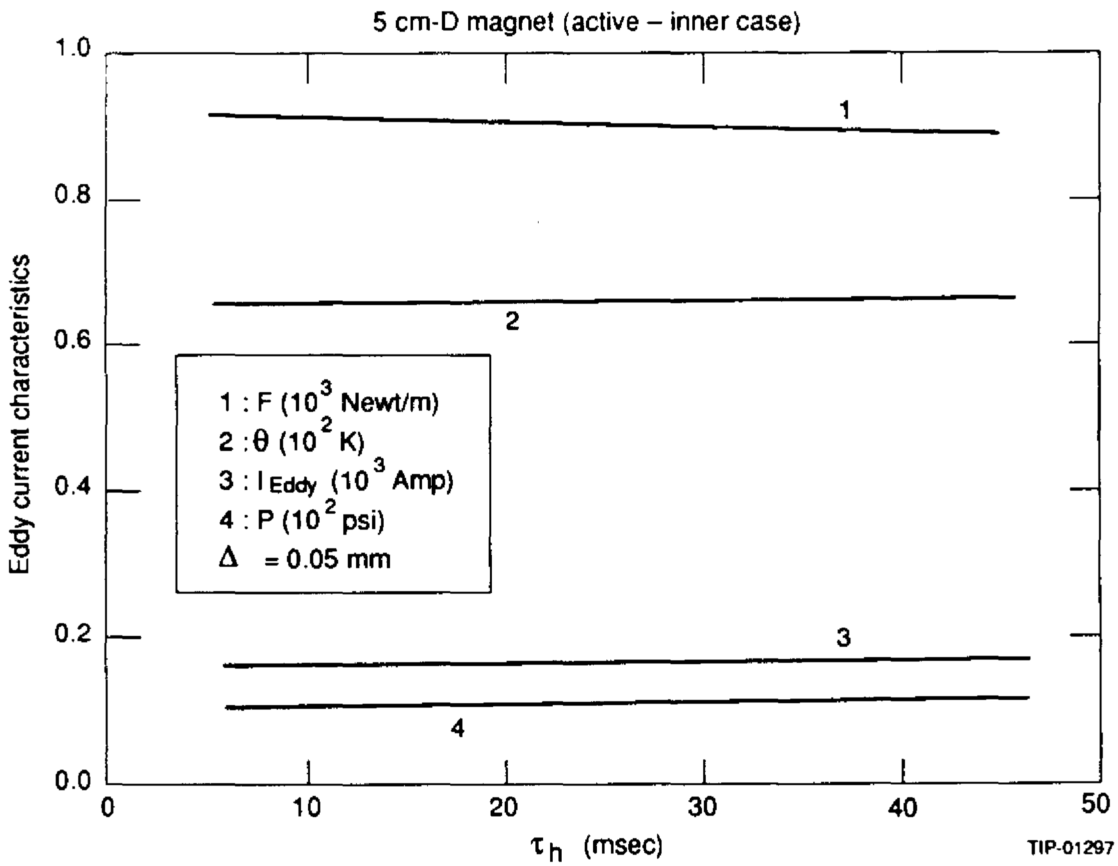

Figure 7. Force per Length Temperature and Eddy Current Induced at the Midplane, and Pressure in a Beam Tube During a Quench in One of the Two Magnets.

6.0 CONCLUSION AND DISCUSSION

The maximum temperature rise is in the beam tube wall, because the eddy currents induced during a quench are not large and occur very late in the quench process (after 0.6 sec). Therefore, there is no reason to expect that this temperature rise will cause other quenches in the same magnet or in the next magnet. The small fraction of the stored energy of the magnet that increases the temperature of the beam pipe is not significant enough to cause a qualitative change in the hot-spot temperature of the coil during a quench.

The peak pressure produced by the Lorentz forces is less than 1 atm (14.696 psi), which is much lower than the pressure produced in the cold mass during a quench[6] ($\geq$ 20 atm);

therefore, the mechanical integrity of the beam tube is not affected by eddy currents. This result suggests that it is even possible to have a copper-plated thickness of 0.1 mm (the peak-pressure would rise to about 2 atm) without having problems with the mechanical integrity of the beam tube.

Neglecting the borders of the magnet, the dependence of Equations (6) and (9) with respect to the angle are exact, but Equation (14) is only a good approximation since heat diffusion along the azimuth direction of the beam tube has been neglected.

The above studies suggests that there is not a significant difference in eddy-current effects, whether a single magnet passive-protection-system or a two magnet active-protection-system is implemented for the SSC ring. Three magnets actively protected were not considered, as the time delay for the magnetic field to collapse is much longer; therefore, it has weaker eddy-current effects.

ACKNOWLEDGEMENTS

I wish to thank Dr. R. Schwitters and Dr. D. Edwards for their support at the SSC Laboratory.

REFERENCES

1. J. D. Jackson, *Classical Electrodynamics*, 2nd edition (Wiley, New York, 1962), Section 6.1.

2. "SSC Conceptual Design," SSC-SR-2020, 1986, Section 4.5.

3. R. B. Meuser, SSC-N-447, 1982; SSC-MAG-99, 1986; R. P. Shutt, BNL Technical Note 53, 1986; A. Chao and J. Peterson, SSC-17, 1985; and C. Haddock, private communication.

4. G. López and G. Snitchler, "Study of Passive and Active Protection System for the SSC R&D Dipole Magnet," SSCL-283, 1990.

5. "SSC Conceptual Design," SSC-SR-2020, 1986, Section 5.5.2.

6. R. P. Shutt, "Estimates of Pressures and Temperatures Generated During Quenches of SSC Magnets," SSC-N-265, 1986.